Early Detection of Bark Beetle Infestation in Norway Spruce (*Picea abies*, L.) using WorldView-2 Data

Markus Immitzer & Clement Atzberger, Vienna, Austria

Summary: In Central Europe and North America, bark beetle infestations cause considerable economic losses. If infested trees are not rapidly removed, large areas can be damaged. Removal of infested trees has to be done during the so-called "green-attack" stage, which is before the bark beetles move to other trees. Field surveys even if they are feasible are cost intensive and impractical if large areas have to be monitored. The aim of the study was to analyse the suitability of 8-band WorldView-2 satellite imagery for detecting bark beetle infestations of two intensity stages (e.g. "dead" and "green-attack") against "healthy" (non-attacked) trees. For classifying individual trees two classifiers, random forest and logistic regression, were evaluated. Despite the relative large class overlap in the spectral signatures, the sample trees (n = 600) could be assigned to the classes "dead", "green-attack", and "healthy" with an overall accuracy of about 75%. Producer's and user's accuracies of all classes were around 70%. The best result was obtained with random forests using the eight spectral bands of a WorldView-2 image acquired in July. With this dataset, an overall accuracy of 76% and a kappa coefficient of 0.61 were achieved. For the separation of the classes "healthy" and "green-attack", vegetation indices based on 2-band normalized differences as well as ratios yielded nearly as good results as the classification with all eight spectral bands. The best results were obtained by combining either the Green or Yellow band with the Near Infrared 1. With regard to individual bands, the Yellow and the Red band are defined as most important ones. We can conclude that 8-band WorldView-2 imagery has the potential for creating hotspot maps of infested trees or of trees with an increased risk of infestation. This could have positive implications for the forest practice.

Zusammenfassung: *Frühzeitige Erkennung von Borkenkäferbefall an Fichten mittels WorldView-2 Satellitendaten*. Borkenkäferepidemien führen in Europa und Nordamerika immer wieder zu großen ökonomischen Verlusten in der Forstwirtschaft. Um großflächige Ausbreitungen zu verhindern, müssen befallene Bäume rasch erkannt und entfernt werden. Die gezielte Entnahme der Bäume, bevor die Käfer ausgeflogen sind, ist schwierig, da die Bäume meist noch keine Verfärbung der Nadeln zeigen. Daher sind derzeit aufwändige und kostenintensive Feldbegehungen notwendig, um eine Ausbreitung des Schädlings zu vermeiden. In dieser Arbeit wurden sehr hochauflösende World-View-2 Satellitendaten mit acht Spektralkanälen von zwei Aufnahmetagen untersucht, um Borkenkäferbefall frühzeitig zu erkennen. Dazu wurde versucht nicht befallene Bäume von befallenen jedoch noch nicht verfärbten („green-attack") und von bereits stark verfärbten bzw. abgestorbenen Bäumen auf Grund der spektralen Reflexion zu trennen. Hierbei wurden die Einzelbaumobjekte mittels Random Forest und Logistischer Regression klassifiziert. Trotz der großen Überschneidungen der spektralen Signaturen zwischen den Klassen „gesund", „befallen – ohne sichtbare Verfärbung" und „abgestorben" konnten diese mit Gesamtgenauigkeiten von rund 75% getrennt werden. Auch die Nutzer- und Produzentengenauigkeiten aller Klassen lagen dabei über 70%. Am besten konnten die Beispielbäume in der Aufnahme vom Juli klassifiziert werden, mit einer Gesamtgenauigkeit von 76% und einem kappa-Wert von 0.61. Zusätzlich wurden verschiedene Vegetationsindizes getestet. Dabei erzielten einzelne normalisierte Differenz- bzw. Verhältnis-Indizes nahezu gleich gute Ergebnisse wie Modelle mit allen acht Spektralkanälen. Die besten Ergebnisse wurden dabei mit Kombinationen des Grün- bzw. Gelb-Kanals mit dem Nahen Infrarot 1 Kanal erreicht. Bei den Modellen basierend auf einzelnen Kanälen brachten der Gelb- bzw. der Rot-Kanal die höchsten Genauigkeiten. Die erzielten Ergebnisse zeigen, dass

im Frühsommer aufgenommene WorldView-2 Szenen Potential für die frühzeitige Erkennung von Borkenkäferbefall aufweisen. Diese Tatsache könnte für die Visualisierung von befallenen Bäumen beziehungsweise von Bäumen mit hohem Befallsrisiko genutzt werden. Solche hotspot-Karten könnten eine große Unterstützung für die forstliche Praxis bei der Bekämpfung von Borkenkäferepidemien darstellen.

1   Introduction

Natural disturbances play an important and often positive role in forest ecosystems. At the same time, however, such disturbances cause great economic damage for forest owners. In Central-European forests windthrow and bark beetles are considered the most important abiotic and biotic disturbance agents in the last century (SCHELHAAS et al. 2003). After the big windthrows in Central Europe in the first ten years of this millennium ("Kyrill" in January 2007, "Paula" in January 2008, and "Emma" in March 2008), beetle infestations in Norway spruce (*Picea abies*, L.) forests increased dramatically (TOMICZEK et al. 2011). Most likely, these problems will increase in the near future. For example, models based on climate change scenarios predict an increasing risk for bark beetle outbreaks (NETHERER & SCHOPF 2010, SEIDL et al. 2011, OVERBECK & SCHMIDT 2012). As Norway spruce is the most valuable tree for European forestry, suitable monitoring methods have to be developed.

In Austria and other European countries, the ecological and economical most relevant bark beetle species are *Ips typographus*, L., and *Pityogenes chalcographus*, L.. Both are on Norway spruce and attack mainly weakened trees. To protect other trees, infested individuals have to be removed before the new larvae are fully developed and start to leave the trees for infesting neighbouring trees. An early detection of infested trees is therefore important to avoid mass outbreaks; best before (visually) discolorations are visible. Usually foresters have to look for early signs of infestation like boring dust around the base of trees (KREHAN 2008). However, a regular large-scale control is too expensive and not practical. Remote sensing techniques are considered useful for an early detection of potentially infested hotspots.

Numerous studies, mainly in North America, pointed out the potential of remote sensing data for detection of (declining) health status of trees. Most of them analysed detection of Mountain Pine Beetles (*Dendroctonus ponderosae*, Hopkins) infestations on Lodgepole Pine (*Pinus contorta*, Dougl.) in Canada. While advanced stages of damage (so called "red-attack" and "grey-attack") can be detected easily, the early detection of an infestation (henceforth referred to as "green-attack") is problematic (ROBERTS et al. 2003, SKAKUN et al. 2003, WULDER et al. 2004, 2006a, 2006b, COOPS et al. 2006). Due to the problems of early detection North American researchers focus their work on the analysis of areas around old "red attack" areas to locate new infestation hot spots (WULDER et al. 2009, COGGINS et al. 2010, 2011).

An early detection of infested trees ("green-attack") would be a major breakthrough regarding the control, prevention and mitigation of large-scale outbreaks. For this reason investigations in the use of remote sensing for detection of infestation before visible discoloration ("green-attack", early detection) continues. HEATH (2001) compared the spectral signatures (compact airborne spectrographic imager – CASI) of healthy, freshly infected ("green-attack") and previously infected ("red-attack") trees and found some trends in the spectra, partially confirming previous studies (e.g., HELLER 1968, HALL 1981). The main problem was the large intra-class variability of the reflectance values hampering the separability of the different infestation classes. Similar results were achieved by SHARMA (2007). For the identification of infestation he characterized the spectral bands between 900 nm and 1100 nm as the most essentially. He concluded that early detection could be possible under certain conditions. CHENG et al. (2010) were able to demonstrate effects of water deficit and changes in chlorophyll content of artificially stressed needles through wavelet analysis of reflection spectra measured in the laboratory. They found good statistical separability in the wavelength ranges between 950 nm and 1390 nm. These results

imply high potential for a cost effective and large-scale method for detection of health status classes of trees.

For the detection of large-scale bark beetle infestation, like in North America, satellite data with low (EKLUNDH et al. 2009) to medium resolution (MEIGS et al. 2011, MEDDENS et al. 2013) can deliver adequate information. For early detection of mostly small-scale infestations in Central Europe the spatial resolution is very important (LAUSCH et al. 2013). With the new generation of very high resolution (VHR) satellite data, multispectral data with spatial resolutions in the metre range are available. MARX (2010) used bi-temporal RapidEye satellite images (mid-April to mid-June) for the detection of bark beetle infested spruce. The first image was used for the separation between spruce stands and deciduous trees. The second image was used for the separation of different attack classes within the spruce stands. In addition to the RapidEye spectral bands, different vegetation indices were included in the analysis. The reference data came from foresters who delineated infested (and healthy) areas in the field. Following experimental set-ups used in North America three infestations classes were classified: "healthy" (= "non-attacked"), "infested" ("green-attack") and "red" ("red-attack"). Classification was done by creating decision tree models. The classification results showed a good separation of the already discoloured trees ("red-attack"). The two classes "healthy" and "infestation" were frequently misclassified. ORTIZ et al. (2013) used RapidEye and TerraSAR-X data, both acquired in May 2009, to detect bark beetle green-attack in southwest Germany. The RapidEye data achieved higher classification accuracies than the SAR data. The highest accuracy was achieved by combining the two datasets.

WorldView-2 data with higher spatial and spectral resolution have also been used for the detection of tree health status. FINNIGAN (2011), for example, used WorldView-2 data for the "red-attack" detection on Lodgepole pine. FILCHEV (2012) tried to map bark beetle stressed spruce in a Bulgarian Biosphere reserve. He used vegetation indices calculated from the eight WorldView-2 spectral bands.

However, the results were not verified with field data.

In addition to satellite data, hyperspectral data from airborne platforms were evaluated for early detection of bark beetle infestations on spruce in several studies. Thereby early stages of infestation ("green-attack") could be detected (FASSNACHT et al. 2012, 2014). LAUSCH et al. (2013) tried to detect very early stages of bark beetle infestation and even forecast infestation with one- or two-year old hyperspectral data. They found a tendency towards detectability of health status; however, they conclude that the achievable accuracies are too low for an application in forestry.

The aim of our study was to analyse the suitability of WorldView-2 imagery for detecting three bark beetle infestation classes on spruce: "dead" (red/grey-attack), "green-attack", and "healthy" (non-attacked) in Central Europe. WorldView-2 is the first commercial satellite providing data with very high spatial (2 m) and spectral (8 bands) resolution. Both factors are important for mapping tree species or health status of individual trees. Since foresters need an early recognition of infested areas remote sensing data were acquired early in summer. For evaluation of the image's acquisition date, data from June and July were tested. Focus was set on identifying relevant spectral bands and vegetation indices for separating the classes "healthy" and "green-attack". The identification of relevant spectral bands has direct implications for practicers as the 4-band version of WorldView-2 data is much cheaper compared to the 8-band version. Ground truth data for the three classes were provided by local foresters through field inspection.

2   Data and Methods

2.1   *Study Site*

The study site covers approximately 1100 ha and is located in central Austria (47°28'N, 14°30'E) in the province of Styria (Fig. 1). The terrain is mountainous and extends from the montane to the subalpin life zone with an elevation ranging from 680 m and 2400 m above sea level. The annual rainfall is between

1250 mm and 1500 mm, with a maximum in July. The bedrocks are mainly base-poor silicates, quartz phyllites and gneisses. The potential natural forest community in the study site is a spruce-fir forest with admixture of beech, larch and sycamore maple (KILIAN et al. 1994). The privately owned forests are commercially used focusing on timber production.

The study site is located next to Enns valley. In this region *Ips typographus*, L. and *Pityogenes chalcographus*, L. are the two most common bark beetle species on spruce. The logging statistics from the year 2010 of Styria reveals a substantial quantity of damaged timber (roughly 1 million cubic metre) caused by bark beetle attacks. This corresponds to approximately one-fifth of the total logging amount of that year. The huge impact of the bark beetle attacks was primarily a late consequence of heavy storm events in the preceeding years ("Kyrill", "Paula" and "Emma") (FACHABTEILUNG 10C DES LANDES STEIERMARK – FORSTWESEN 2011).

2.2 *WorldView-2 Data*

The WorldView-2 satellite provides very high spatial resolution data with eight spectral bands. At nadir the ground resolution (GSD) is 50 cm for the panchromatic band (0.46 µm – 0.80 µm) and 200 cm for the multispectral bands. In addition to the four standard bands Blue (0.45 µm – 0.51 µm), Green (0.51 µm – 0.58 µm), Red (0.63 µm – 0.69 µm), and Near Infrared 1 (NIR 1, 0.77 µm – 0.90 µm), another four bands are available. The four additional bands are Coastal (0.40 – 0.45 µm), Yellow (0.59 µm – 0.63 µm), Red Edge (0.71 µm – 0.75 µm), and Near Infrared 2 (NIR 2, 0.86 µm – 1.04 µm). Further details about the sensor can be found on the website of the provider (DIGITAL GLOBE 2014) and in UPDIKE & COMP (2010). WorldView-2 data can be ordered either with the four conventional bands or (at higher costs) with all eight bands. The good suitability of WorldView-2 for tree species classification has already been shown (IMMITZER et al. 2012a, WASER et al. 2014).
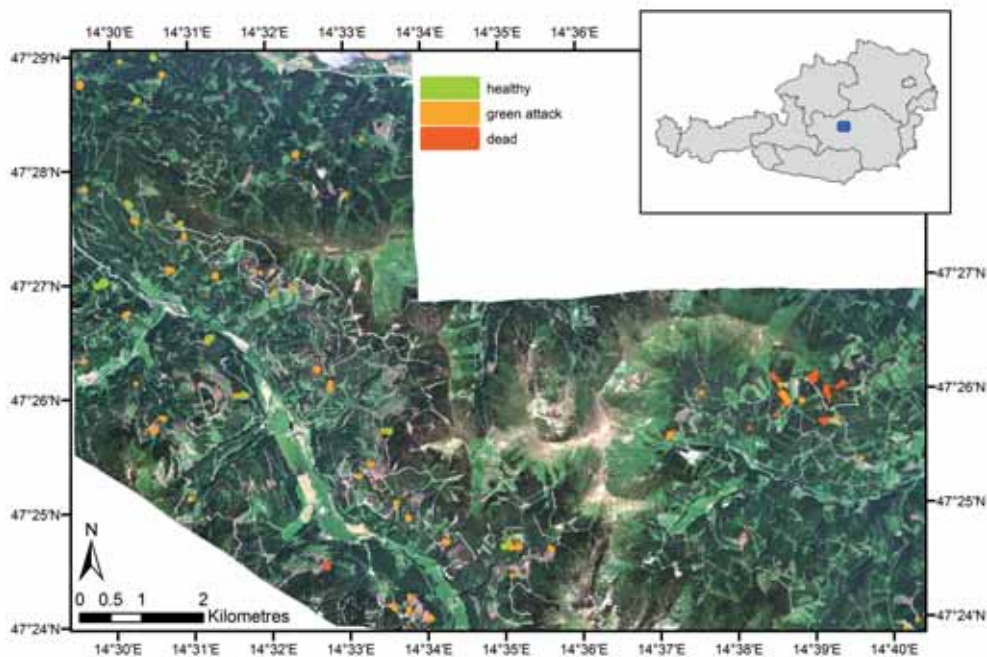

Fig. 1: WorldView-2 image (true-colour composite with the bands Red, Green, Blue) of the study site from June 2010. The locations of the reference data are shown in green ("healthy"), orange ("green-attack") and red ("dead"). The inlet indicates the position (blue) of the study site in the province of Styria in Austria.

For the purpose of the study, three World-View-2 images with eight bands and processing level "Ortho Ready Standard" were obtained. The first image was acquired in June 2010. At that time the first generation of bark beetle was fully developed. The second image was taken in July and third in October, at the end of the growing season. All scenes were recorded under cloudless conditions over the study site. Detailed recording parameters can be found in Tab. 1. The third image was only used for confirming the location of reference data identified during field work. An image acquisition in October would be too late for early detection of "green-attack". Hence, only the two summer images (June and July 2010) were used for the classification exercise.

Before data analysis, the two summer scenes were atmospherically corrected, pansharpened and orthorectified. To derive top-of-canopy reflectance, the pixel gray values (digital numbers) were first converted into spectral 'at-sensor' radiance (UPDIKE & COMP 2010) using the ENVI module (ENVI 4.8) FLAASH. The settings were chosen iteratively by checking the resulting reflectance values for plausibility. Optimal results were obtained with the following FLAASH settings: Atmospheric Model: Mid-Latitude Summer, Aerosol Model: Rural, Initial Visibility: 60 km (June) and 70 km (July). The atmospheric correction resulted in meaningful spectral reflectance signatures of the tree crowns. For visualisation purposes a pansharpening was performed to enhance the spatial resolution of the eight multispectral bands. Therefore, the HCS (Hyperspherical Color Space) algorithm (PADWICK et al. 2010) implemented in ERDAS Imagine was used. Finally, both images, with 2 m and 0.5 m were orthorectified using a digital terrain model (5 m grid) and about 20 ground control points per scene. The coordinates of the control points were taken from a colour-infrared orthophoto with 0.5 m pixel size. The achieved average accuracy (RMSE) was about 1.8 pixels on images with 2 m pixel size.

2.3 Reference Data

As reference information we used groups of infested and healthy trees identified by experienced local forest staff through field inspections in the summer months. The tree groups were surveyed with GPS and marked on orthophotos. In most cases, the two classes were located near each other. So systematic differences in slope and azimuth (and consequently in illumination conditions) between the two classes can be excluded. Some of the infested trees were discoloured over the acquisition period. Others showed no visual changes between summer and autumn images. Most of the infested tree groups, however, were harvested by the foresters before the third image was acquired to prevent large-scale outbreaks.

Within the study we assumed that infestation by bark beetle (*Ips typographus*, L.) caused the discoloration of the trees. The trees were typically attacked early in spring or in the previous year. Healthy and infected trees display no visible differences in the true colour composites of the summer images (Fig. 2). Trees that are clearly discoloured in the summer images (June, July) were assigned to the class "dead" (red/grey-attack). We assume that these trees were attacked by bark beetle in one of the previous years and were already dead or almost dead in 2010. Fig. 2 shows sample images of the three data acquisition dates for the three infestation classes.

Tab. 1: Recording parameters of the three WorldView-2 images.

	June	July	October
Acquisition date	12 June 2010	10 July 2010	11 October 2010
Scan direction	reverse	forward	forward
Mean satellite elevation	76.8°	65.6°	66.7°
Mean satellite azimuth	159.1°	135.5°	7.6°
Mean off nadir view angle	11.8°	21.4°	20.9°

Based on the reference polygons from field inspections and the two summer scenes, we selected in total about 600 reference trees within each image. In the June scene we manually delineated 257 "healthy", 272 "green-attacked", and 81 "dead" trees. In the July image 256 "healthy", 245 "green-attack", and 79 "dead" trees were identified. For each reference tree, we manually delineated the well-illuminated part of the tree crown to minimize shadow effects (CLARK et al. 2005, LECKIE et al. 2005, GREENBERG et al. 2006, IMMITZER et al. 2012a). It was not possible to automate the tree crown delineation because of strongly varying acquisition geometries.

To locate the sample trees, the pansharpened image with 0.5 m pixel size was displayed together with the multispectral image with 2 m pixel size both as colour-infrared composite (RGB: NIR 1, Red and Green). Then we selected the sun-lit pixels per tree crown in the multispectral image with 2 m pixel size and converted them to a polygon vector file. Finally, this file was used for extracting the spectral information from the corresponding World-View-2 image. This workflow allowed a rapid
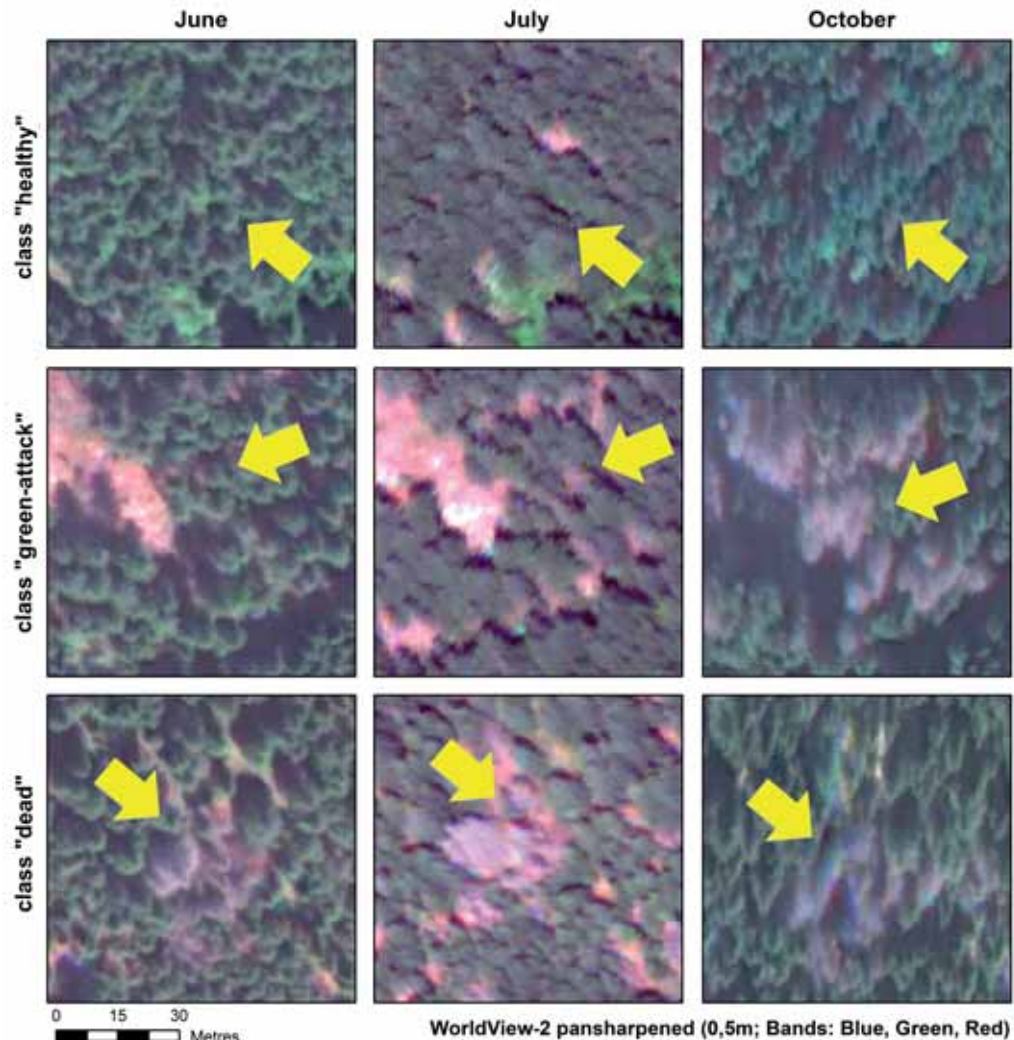

Fig. 2: Examples (marked with yellow arrows) of the three infestation classes ("healthy", "green-attack" and "dead") on pansharpened and atmospherically corrected summer and autumn World-View-2 images.

selection and pixel-sharp demarcation of tree crowns (IMMITZER et al. 2012b).

2.4 *Spectral Separation and Classification of Infestation Classes*

Based on the manually delineated tree crowns (section 2.3), the spectral values in the eight WorldView-2 bands were extracted and analysed. The mean values for each crown polygon were calculated and used for further analysis.

For separating the three infestation classes, we used the non-parametric, ensemble learning random forest (RF) classifier (BREIMAN 2001). The RF classifier is increasingly used for the classification of remote sensing data (PAL 2005, IMMITZER et al. 2012a, RODRÍGUEZ-GALIANO et al. 2012). Some of the advantages of this method are (I) it does not make any assumptions about data distribution and the collinearity in the data, (II) it does not require common covariance in the classes, (III) thanks to the integrated bootstrapping the accuracy estimates are obtained from independent samples, and (IV) it provides variable importance measures which can be helpful for feature selection (BREIMAN 2001, LIAW & WIENER 2002, HASTIE et al. 2009, IMMITZER et al. 2012a, TOSCANI et al. 2013). In our study, the following parameterization of the RF was used: 500 trees and two variables at each node (= the square-root of the total number of input variables) at each node. We created models using all eight, respectively, the four conventional WorldView-2 bands (Blue, Green, Red and NIR 1). We analysed the 2- and 3-class separability.

Although RF provides variable importance measures, logistic regression (LR) was used as an additional method to identify the most important spectral bands for separating the two most similar classes "green-attack" and "healthy". One advantage of LR is that models can also be built with only one explanatory variable, which is not meaningful with a decision tree-based method like RF. The drawback of LR is that it can only handle two-class problems. Using LR, we first created models with all eight spectral bands (baseline) and then with the four conventional ones. Next, every single band was used individually.

In addition to the eight spectral bands, we tested three categories of vegetation indices (Tab. 2), similar to other studies (BUSCHMANN & NAGEL 1993, GITELSON & MERZLYAK 1994, SIMS & GAMON 2002, MARX 2010). Within each category, all possible band combinations were tested. The first group of indices was obtained by calculating the difference and the second by calculating the ratio of two WorldView-2 bands, respectively. Analogously to the formula of the widely used NDVI (normalized difference vegetation index) (ROUSE et al. 1973), normalized differences were calculated as a third group, again using all possible permutations.

To build LR models, we used bootstrap samples (random sampling with replacement) drawn from the original dataset (EFRON 1979). With the generated model all undrawn samples were classified and the classification accuracy was then calculated. We repeated this procedure 500 times and used the majority votes of the iterations.

To evaluate the results of RF and LR we produced confusion matrices with the majority vote from all bootstrap iterations and calculated the producer's and user's accuracies for each class, the overall accuracy (correct classification rate), and Cohen's kappa coefficient (COHEN 1960).

For modelling R 3.0.2 (R CORE TEAM 2013) was applied with the additional packages MASS (VENABLES & RIPLEY 2002), randomForest (LIAW & WIENER 2002), and caret (KUHN et al. 2013).

Tab. 2: Formulas for indices calculation: R_x and R_y denote reflectance values of two different WorldView-2 bands. All possible permutations were tested. The indices were evaluated by logistic regression.

Index type	Index formula
Difference indices	$R_y - R_x$
Ratio indices	$\dfrac{R_x}{R_y}$
Normalised difference indices	$\dfrac{R_y - R_x}{R_y + R_x}$

3 Results

3.1 *Spectral Signatures*

Fig. 3 shows the spectral signatures of the three infestation classes based on the July scene. The class "dead" shows higher reflectance values in the visible wavelength range and lower values in the near infrared compared to the two other classes. The differences between the classes "green-attack" and "healthy" are much smaller. The mean value of the class "green-attack" often lies between the average signatures of the two other classes. The largest distinctions between the classes "healthy" and "green-attack" appeared in the bands Yellow and Red. However, we found high within-class variances in all classes leading to significant class overlaps.

3.2 *Results of the Random Forest Classifier for the three Infestation Classes*

The RF classification of the three infestation classes based on the spectral data (all eight bands) produced very similar results for the two summer images: the overall accuracy with the June image was 74.4%, and with the July image 76.2%. Kappa coefficient was around 0.60 for both classifications. The con-
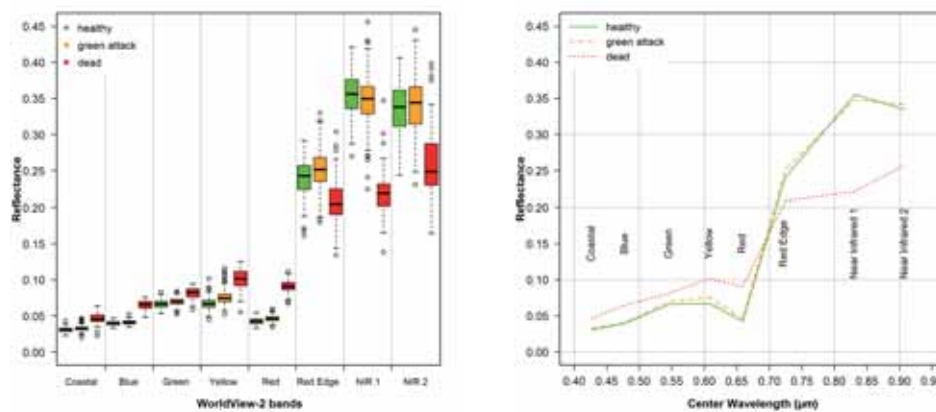

Fig. 3: Reflectance values of the three infestation classes "healthy", "green-attack" and "dead" based on the WorldView-2 image acquired on 10th July 2010: (a) boxplots and (b) spectral signatures (median values).

Tab. 3: Confusion matrix for the three classes "healthy", "green-attack", and "dead" using all eight bands of the WorldView-2 images from June and July, respectively, and the random forest classifier (independent bootstrapping results).

| | Field data | | | | | | | | | |
| | healthy | | green-attack | | dead | | Σ | | User's acc. | |
Classified as	June	July	June	July	June	July	June	July	June	July
Healthy	167	185	65	67	0	0	232	79	0.720	0.734
Green-attack	90	71	207	178	1	0	298	249	0.695	0.715
Dead	0	0	0	0	80	79	80	252	1.000	1.000
Σ	257	256	272	245	81	79	610	580		
Producer's acc.	0.650	0.723	0.761	0.727	0.988	1.000	Overall acc.		0.744	0.762

fusion matrices in Tab. 3 show that the class "dead" can be nearly perfectly separated from the two other classes. Producer's (PA) and user's accuracy (UA) for the class "healthy" was for the two images in the order of ≥ 72% (except PA for June image: 65.0%). Similar values were obtained for the class "green-attack", with however somewhat higher PA (73% – 76%) and lower UA (70% – 72%). Between the two summer images, only small differences could be detected. The PA of the July image was higher for the class "healthy" (72.3% vs. 65.0%) and for the class "green-attack" lower (76.1% vs. 72.7%) compared to the June image.

The use of the four conventional bands instead of all eight bands resulted in a decrease of classification accuracy for both images. The obtained overall accuracy for June was 71.6% (kappa 0.53) and those for July 70.2% (kappa 0.51).

3.3 *Separation of the Classes "Healthy" and "Green-attack"*

The bootstrapped results using RF and LR for separating the classes "healthy" and "green-attack" are shown in Tab. 4 to Tab. 8. The colours indicate the level of accuracy (based on

kappa coefficients), increasing from white to green. As expected, the models without the easily separable class "dead", showed lower classification accuracies compared to the 3-class problem. Using all eight bands, both classes "healthy" and "green-attack" could be correctly assigned with an accuracy of around 70% with both approaches (RF and LR) and both images. The models based on the four conventional bands showed generally lower classification precision, except the LR model using the June data (Tab. 4).

The models with single spectral bands achieved significantly lower results, particularly for the June image (Tab. 5). When assessed individually, the Red and Green bands were most significant in the June image. In the July image, the drop in accuracy was less pronounced. Here, the Yellow band showed the highest accuracy, closely followed by the Red band. The two bands almost reached an accuracy of 70%, which is comparable with those of the LR models with the four conventional bands. For both summer images, the worst results were obtained using solely the bands in the near infrared. The Red Edge band had little discriminative power when used alone.

The results obtained from LR models using single bands could be confirmed with the two importance measures derived from RF model

Tab. 4: Overall accuracies and corresponding kappa coefficients (in brackets) from random forest (RF) and logistic regression (LR) models to separate "healthy" and "green-attack" samples using all eight and the four conventional spectral bands of WorldView-2 images acquired in June and July (independent bootstrapping results).

	RF – eight bands	RF – four bands	LR – eight bands	LR – four bands
June	0.703 (0.405)	0.682 (0.364)	0.713 (0.424)	0.726 (0.451)
July	0.737 (0.473)	0.659 (0.318)	0.711 (0.424)	0.693 (0.384)

Tab. 5: Overall accuracies and corresponding kappa coefficients (in brackets) from logistic regression models to separate "healthy" and "green-attack" samples using single bands of the WorldView-2 images acquired in June and July (independent bootstrapping results).

	Coastal	Blue	Green	Yellow	Red	Red Edge	NIR 1	NIR 2
June	0.493 (-0.036)	0.631 (0.260)	0.656 (0.311)	0.626 (0.250)	0.658 (0.315)	0.531 (0.056)	0.518 (0.031)	0.484 (-0.048)
July	0.583 (0.164)	0.565 (0.127)	0.635 (0.269)	0.693 (0.384)	0.669 (0.337)	0.575 (0.149)	0.543 (0.082)	0.523 (0.043)

Tab. 6: Overall accuracies and corresponding kappa coefficients (in brackets) from logistic regression models to separate "healthy" and "green-attack" samples using difference indices from the WorldView-2 images acquired in July (below the diagonal) and in June (above the diagonal), (independent bootstrapping results).

Band	Coastal	Blue	Green	Yellow	Red	Red Edge	NIR 1	NIR 2
Coastal	-	0.643 (0.284)	0.648 (0.295)	0.628 (0.254)	0.643 (0.284)	0.520 (0.034)	0.533 (0.062)	0.497 (-0.021)
Blue	0.511 (0.018)	-	0.624 (0.246)	0.567 (0.131)	0.624 (0.246)	0.503 (-0.004)	0.505 (0.000)	0.486 (-0.057)
Green	0.551 (0.099)	0.593 (0.185)	-	0.539 (0.075)	0.539 (0.073)	0.482 (-0.064)	0.473 (-0.082)	0.469 (-0.077)
Yellow	0.699 (0.396)	0.667 (0.332)	0.653 (0.304)	-	0.471 (-0.086)	0.467 (-0.091)	0.473 (-0.071)	0.457 (-0.111)
Red	0.603 (0.203)	0.661 (0.320)	0.499 (-0.011)	0.637 (0.272)	-	0.474 (-0.078)	0.474 (-0.069)	0.454 (-0.117)
Red Edge	0.559 (0.117)	0.575 (0.148)	0.569 (0.136)	0.507 (0.007)	0.557 (0.112)	-	0.478 (-0.066)	0.478 (-0.056)
NIR 1	0.551 (0.099)	0.561 (0.119)	0.585 (0.167)	0.615 (0.228)	0.581 (0.159)	0.681 (0.361)	-	0.514 (0.020)
NIR 2	0.505 (0.005)	0.505 (0.006)	0.499 (-0.009)	0.471 (-0.074)	0.495 (-0.018)	0.517 (0.029)	0.597 (0.194)	-

Tab. 7: Overall accuracies and corresponding kappa coefficients (in brackets) from logistic regression models to separate "healthy" and "green-attack" samples using ratio indices from the WorldView-2 images acquired in July (below the diagonal) and in June (above the diagonal) (independent bootstrapping results).

Band	Coastal	Blue	Green	Yellow	Red	Red Edge	NIR 1	NIR 2
Coastal	-	0.616 (0.232)	0.597 (0.194)	0.618 (0.234)	0.631 (0.262)	0.509 (0.010)	0.507 (-0.001)	0.480 (-0.067)
Blue	0.547 (0.091)	-	0.586 (0.169)	0.535 (0.066)	0.629 (0.257)	0.539 (0.074)	0.582 (0.162)	0.577 (0.151)
Green	0.507 (0.002)	0.533 (0.063)	-	0.501 (-0.026)	0.599 (0.198)	0.597 (0.195)	0.707 (0.412)	0.637 (0.274)
Yellow	0.627 (0.253)	0.671 (0.340)	0.647 (0.293)	-	0.550 (0.098)	0.654 (0.307)	0.62 (0.236)	0.648 (0.295)
Red	0.547 (0.090)	0.649 (0.296)	0.639 (0.277)	0.543 (0.083)	-	0.641 (0.28)	0.694 (0.385)	0.671 (0.341)
Red Edge	0.523 (0.037)	0.497 (-0.014)	0.521 (0.030)	0.663 (0.323)	0.581 (0.158)	-	0.488 (-0.044)	0.535 (0.063)
NIR 1	0.621 (0.238)	0.607 (0.211)	0.683 (0.364)	0.711 (0.419)	0.689 (0.376)	0.687 (0.372)	-	0.480 (-0.054)
NIR 2	0.553 (0.101)	0.501 (-0.008)	0.567 (0.129)	0.667 (0.331)	0.603 (0.202)	0.583 (0.163)	0.577 (0.155)	-

(8 bands, 2 classes). Both importance measurements ("mean decrease in Gini" and "mean decrease in accuracy") ranked the Red and the Green band as the most important variables using the June image. For the July image the two top ranked bands were Yellow and Red.

Classification accuracies obtained by using difference indices are reported in Tab. 6 to Tab. 8. Only results for one band order are shown (wavelength band y > wavelength band x), as differences were either inexistent (difference and normalized difference indices) or very small (ratio indices).

Compared to the use of single spectral bands, the classification accuracy from difference indices was either stable (June) or slightly improved (July). Only few models show better results than a purely random model (kappa coefficient > 0). For both images, difference indices employing the Coastal band gave highest accuracies.

The use of ratios instead of differences between two spectral bands improved the separability of the two infestation classes (Tab. 7). Most of the models, however, showed very low kappa-values which denote unsatisfied

model accuracy. Band ratios combining Near Infrared 1 with Green (June), respectively Yellow (July) resulted in mean overall accuracies nearly similar to models using all eight spectral bands. These models proofed significant (kappa values > 0.4). Comparable results were also obtained using normalized differences (Tab. 8). Again, combining bands in the near infrared with the bands Green or Red yielded best results. In the July image, Near Infrared 1 combined with Yellow performed also very well.

4   Discussion

In our study the WorldView-2 data showed the potential to detect spectral differences between "healthy" and bark beetle infected "green-attack" trees. However, the spectral differences between the two infestation classes are small and blurred by high within-class variances. As a result, classification accuracies (RF and LR) do not exceed 70% for these two classes. Studies using hyperspectral data also found significant overlaps between

Tab. 8: Overall accuracies and corresponding kappa coefficients (in brackets) from logistic regression models to separate "healthy" and "green-attack" samples using normalized difference indices from the WorldView-2 images acquired in July (below the diagonal) and in June (above the diagonal) (independent bootstrapping results).

Band	Coastal	Blue	Green	Yellow	Red	Red Edge	NIR 1	NIR 2
Coastal	-	0.611 (0.220)	0.605 (0.207)	0.62 (0.236)	0.635 (0.268)	0.514 (0.020)	0.507 (-0.002)	0.51 (-0.008)
Blue	0.551 (0.100)	-	0.582 (0.160)	0.543 (0.079)	0.635 (0.268)	0.533 (0.066)	0.571 (0.141)	0.567 (0.135)
Green	0.505 (-0.002)	0.537 (0.071)	-	0.509 (-0.011)	0.601 (0.202)	0.582 (0.166)	0.705 (0.409)	0.633 (0.268)
Yellow	0.627 (0.253)	0.675 (0.348)	0.641 (0.280)	-	0.558 (0.112)	0.652 (0.304)	0.637 (0.273)	0.643 (0.285)
Red	0.547 (0.090)	0.649 (0.296)	0.637 (0.272)	0.543 (0.084)	-	0.618 (0.237)	0.682 (0.364)	0.673 (0.347)
Red Edge	0.521 (0.033)	0.497 (-0.013)	0.521 (0.030)	0.663 (0.323)	0.581 (0.158)	-	0.469 (-0.081)	0.535 (0.065)
NIR 1	0.621 (0.238)	0.607 (0.211)	0.683 (0.364)	0.709 (0.415)	0.699 (0.396)	0.689 (0.377)	-	0.509 (0.008)
NIR 2	0.553 (0.101)	0.503 (-0.004)	0.569 (0.133)	0.675 (0.347)	0.603 (0.202)	0.579 (0.155)	0.595 (0.190)	-

the two most problematic infestation classes (Heath 2001, Lausch et al. 2013). On the contrary, in our study, the class of "dead" trees could be classified almost perfectly.

Despite the relatively large class overlap in the spectral signatures, the manually delineated trees could be assigned to the classes "dead", "green-attack", and "healthy" by supervised classification (random forests, RF) with an overall accuracy of about 75%. The producer's and user's accuracies of all classes were around 70%. The best result was obtained with RF using all eight spectral bands of the July image. With this dataset, an overall accuracy of 76.2% and a kappa coefficient of 0.609 were achieved. Using only the four conventional WorldView-2 bands (Blue, Green, Red and Near Infrared 1) generally resulted in a loss of discriminative power. For the separation of the classes "green-attack" and "healthy" using RF or logistic regression (LR) the best results were achieved with all eight bands. Only the LR model using the June data was an exception. This might be due to the fact that unsuitable variables can worsen a LR model, whereas RF can handle this.

The similar accuracies of the classes "green-attack" and "healthy" is maybe caused by the equal data distribution between these two classes in the reference data. In a real-world setting, the occurrence of the class "healthy" is usually considerably higher than those of the infested trees. As we had no a priori information regarding the class distribution within our study area, we opted for an equal sampling of the three classes. Possible errors in the reference data have also to be taken into account when interpreting our results.

Using RapidEye data, Marx (2010) was able to separate the three classes with an overall accuracy of 98.6%. However, in this study, 97% of the samples were healthy trees, thus euphemising the overall accuracy. Looking at the results for the classes "green-attack" and "dead" the accuracies of our study are in line with or even higher than those found by Marx (2010). The "green-attack" trees were classified by Marx (2010) with a user's accuracy of 76.5% and with a producer's accuracy of 40.9%, the values for "red-attack" (nearly equivalent to our class "dead") were 87.4% and 80.2%, respectively. Our results

also outperform those of Ortiz et al. (2013) using RapidEye data for the green-attack detection. The user's and producer's accuracies in their study were 50.0% and 66.7%, respectively. The higher accuracies in our study may be due to the higher spatial resolution of the WorldView-2 images (2 m) compared with the RapidEye data (5 m). It has also to be noted that we only classified the well illuminated parts of the tree crowns. The high detectability of already advanced stages of bark beetle infestation based on WorldView-2 data is also consistent with the results from Finnigan (2011).

A question arising in bark beetle studies is whether the remote sensing data detects directly the infested trees or solely a certain pre-weakening. This pre-weakening of trees could increase the predisposition to bark beetle infestation. The detection of pre-weakening of spruces was also highlighted in the study by Lausch et al. (2013). They used one- and two-year old hyperspectral data to classify different infestation classes. Their best model achieved very similar results as our study. They classified the three classes "dry" (old bark beetle infestations), "infestation 2010" and "healthy" with an overall accurcy of 69.3% (kappa 0.54) using hyperspectral HyMap data from 2009. The user's and producer's accuracies of the class "dry" were nearly 90%, those of the other classes were around 60%, therefore, the infestation of 2010 could be forcasted with data from 2009.

With respect to the image acquisition date, we found only small differences between the June and July images. The accuracies obtained from 8-band RF classification in the June image were almost as good as the July image. Using LR and various 2-band vegetation indices, the June image gave only slightly lower accuracies compared to the July image. An early image acquisition as such in June would give the forest practitioners extra time to remove infested trees before the bark beetles spread out. However, this requires good acquisition conditions, e.g. cloud free conditions with low haze levels and near-nadir view angles. In practice, one recommendation could be to task an early image acquisition, e.g. June, but insisting on optimum conditions. If these cannot be met the acquisition window should be

extended, e.g. into July, until suitable weather conditions are encountered.

Remarkably, for the separation of the classes "healthy" and "green-attack", some vegetation indices based on 2-band normalized differences and ratios yielded nearly as good results as the classification with all eight spectral bands. The best results were obtained with the bands Green and Near Infrared 1 from the June image and Yellow and Near Infrared 1 from the July image, respectively. The new bands Red Edge and Near Infrared 2 achieved significantly worse results. The use of spectral indices does not only permit an easy visualization of data compared to eight band data but also results in a simplified modelling, significantly reducing the necessary computer power and storage requirements. Possibly, the usage of 2-band vegetation indices reduces negative impacts related to illumination differences and topographic effects. However, these aspects were not studied in the present work.

Numerous studies identified bands from the green peak up to the Red Edge region as relevant for an early detection of plant stress induced by bark beetle infestation or air pollution (Stone et al. 2001, Lawrence & Labus 2003, Entcheva Campbell et al. 2004, Fassnacht et al. 2012, 2014, Lausch et al. 2013). This was also confirmed by our investigation, where the bands Red / Green (June) and Yellow / Red (July) showed the highest prediction power in the models with single bands. The same bands were identified by RF as the most important ones. In our study however, the Red Edge band was amongst the worst performing bands within the visible spectral range.

Regarding alternative data sources, World-View-2 images have a few advantages compared to classical aerial images as well as hyperspectral datasets. One advantage of World-View-2 data compared to hyperspectral imagery is its higher spatial resolution and large-scale mapping capacity. Lausch et al. (2013), for example, identified a problem of mixed information using hyperspectral data with a spatial resolution of 4 m. In their study it was pointed out that a spatial resolution of about 1 m would be interesting for mapping purposes at tree level. On the other hand, imaging spectroscopy certainly permits the detection of more subtle absorption features, which

are not present in the rather coarse bands of the WorldView-2 sensor (Schlerf et al. 2010). Aerial images usually have a very high spatial resolution and are clearly cheaper than World-View-2 data. But the number of spectral bands is smaller and radiometric inhomogeneity in the data makes large-scale applications difficult. However, it still has to be checked if the four additional WorldView-2 bands are more beneficial for the early detection of bark beetle infestation or the higher spatial resolution of aerial images. Aside from data with high spectral and high spatial resolution, multi-temporal data (Meigs et al. 2011, Meddens et al. 2013) as well as multi-sensor data (Ortiz et al. 2013) can increase classification accuracy.

5   Conclusion and Outlook

The study showed that WorldView-2 satellite data may be useful for large-scale applications aiming at the detection of advanced as well as early bark beetle infestation with remote sensing data. However, the data does not permit to reliably identify each tree at the "green-attack" stage of infestation. Nonetheless, the data might be suitable to create hotspot maps of infested trees and of trees with an increased risk of infestation. Such maps would be an important information gain for the forest practice and would probably lead to an increase in efficiency of bark beetle infestation control.

Remotely sensed maps of bark beetle infestation could also positively contribute to the bark beetle modelling community. Both, the information from advanced bark beetle infestation (dead trees) with high confidence level, as well as the less reliable information from green-attack trees could constitute essential input data in bark beetle models. For example, it can be expected that the combination of maps showing green-attack and dead trees with predisposition models (Netherer & Nopp-Mayr 2005) could increase the prediction accuracy of such models. Remotely sensed maps can also be used as an alternative to cost intensive inventory data for detailed GIS modelling approaches of bark beetle infestation similar to the work described in Rossi et al. (2009).

With respect to our methodology, the spectral separability, positioning of reference polygons on the image, processing time and data volume needs further analysis. For further studies, it is also recommended to improve the collection of reference data. A more precise localisation of the trees in the field or a delineation of the individual crowns on the remote sensing images would make the localization of the trees less time consuming. In addition, a detailed description of the infestation stage, such as boring dust emission, start of the tree crown discoloration, and so on, would be helpful.

It was shown that mainly the four conventional bands (Blue, Green, Red and Near Infrared 1) and derived indices positively contributed to the separation of the infestation classes. Amongst the four new bands of WorldView-2, only the Yellow band had importance. For this approach it would be interesting to analyse the potential of other remote sensing data, e.g. digital aerial images. Furthermore, the potential of spectral regions not covered by the WorldView-2 satellite should be analysed. Therefore, for further studies applying hyperspectral data with very high spatial resolution is recommended. In this way, one could also test newer parameterizations of the Red Edge feature for detecting bark beetle infestation classes (Cho et al. 2008). In our study, the so-called Red Edge band of World-View-2 did not positively contribute to the class separability.

This study and previous studies on tree species discrimination (Immitzer et al. 2012a, 2012b) have shown that the classification accuracy can be increased, if only the well-lit parts of the crowns are used. So far, the delineation of the crown has been made manually. For an operational, large-scale application this procedure must be automated. Initial tests of different segmentation algorithms were promising but not yet used.

The bulk of the above mentioned suggestions are addressed in an actual joint research project together with Bavarian State Institute of Forestry (LWF), German Aerospace Center (DLR), Bavaria State Forest Enterprise (BaySF) and Austrian State Forest Enterprise (ÖBf) with study areas in Bavaria and Austria. We are planning detailed analyses of time series both of WorldView-2 and airborne hyperspectral data (HySpex) with very high spatial resolution for observing vitality loss of artificially stressed trees.

Acknowledgements

References

Breiman, L., 2001: Random forests. – Machine learning **45** (1): 5–32.

Buschmann, C. & Nagel, E., 1993: In vivo spectroscopy and internal optics of leaves as basis for remote sensing of vegetation. – International Journal of Remote Sensing **14** (4): 711–722.

Cheng, T., Rivard, B., Sánchez-Azofeifa, G.A., Feng, J. & Calvo-Polanco, M., 2010: Continuous wavelet analysis for the detection of green attack damage due to mountain pine beetle infestation. – Remote Sensing of Environment **114** (4): 899–910.

Cho, M.A., Skidmore, A.K. & Atzberger, C., 2008: Towards red-edge positions less sensitive to canopy biophysical parameters for leaf chlorophyll estimation using properties optique spectrales des feuilles (PROSPECT) and scattering by arbitrarily inclined leaves (SAILH) simulated data. – International Journal of Remote Sensing **29** (8): 2241–2255.

Clark, M.L., Roberts, D.A. & Clark, D.B., 2005: Hyperspectral discrimination of tropical rain forest tree species at leaf to crown scales. – Remote Sensing of Environment **96** (3-4): 375–398.

Coggins, S.B., Coops, N.C. & Wulder, M.A., 2010: Improvement of low level bark beetle damage estimates with adaptive cluster sampling. – Silva Fennica **44** (2): 289–301.

Coggins, S.B., Coops, N.C. & Wulder, M.A., 2011: Estimates of bark beetle infestation expansion factors with adaptive cluster sampling. – International Journal of Pest Management **57** (1): 11–21.

Cohen, J., 1960: A coefficient of agreement for nominal scales. – Educational and Psychological Measurement **20** (1): 37–46.

Coops, N.C., Johnson, M., Wulder, M.A. & White, J.C., 2006: Assessment of QuickBird high spatial resolution imagery to detect red attack damage due to mountain pine beetle infestation. – Remote Sensing of Environment **103** (1): 67–80.

Digital Globe, 2014: White Paper – The benefits of the 8 spectral bands of WorldView-2. – http://digitalglobe.com/ (7.7.2014).

Efron, B., 1979: Bootstrap Methods: Another Look at the Jackknife. – The Annals of Statistics **7** (1): 1–26.

Eklundh, L., Johansson, T. & Solberg, S., 2009: Mapping insect defoliation in Scots pine with MODIS time-series data. – Remote Sensing of Environment **113** (7): 1566–1573.

Entcheva Campbell, P.K., Rock, B.N., Martin, M.E., Neefus, C.D., Irons, J.R., Middleton, E.M. & Albrechtova, J., 2004: Detection of initial damage in Norway spruce canopies using hyperspectral airborne data. – International Journal of Remote Sensing **25** (24): 5557–5583.

Fachabteilung 10C des Landes Steiermark – Forstwesen, 2011: Fichtenborkenkäfersituation 2011. – http://www.agrar.steiermark.at/cms/beitrag/10435428/12717247/ (4.9.2011).

Fassnacht, F.E., Latifi, H. & Koch, B., 2012: An angular vegetation index for imaging spectroscopy data – Preliminary results on forest damage detection in the Bavarian National Park, Germany. – International Journal of Applied Earth Observation and Geoinformation **19**: 308–321.

Fassnacht, F.E., Latifi, H., Ghosh, A., Joshi, P.K. & Koch, B., 2014: Assessing the potential of hyperspectral imagery to map bark beetle-induced tree mortality. – Remote Sensing of Environment **140**: 533–548.

Filchev, L., 2012: An Assessment of European Spruce Bark Beetle Infestation Using WorldView-2 Satellite Data. – European SCGIS Conference "Best practices: Application of GIS technologies for conservation of natural and cultural heritage sites", Sofia, Bulgaria.

Finnigan, L., 2011: Evaluating the Utility of Eight Band Worldview-2 Imagery in the Detection of Red Attack. 8-Band Research Challenge, DigitalGlobe. – http://dgl.us.neolane.net/res/img/bee83c5d3c55789b4bf6f23e4f309a8a.pdf (16.1.2012).

Gitelson, A. & Merzlyak, M.N., 1994: Spectral reflectance changes associated with autumn senescence of Aesculus hippocastanum L. and Acer platanoides L. leaves. Spectral features and relation to chlorophyll estimation. – Journal of Plant Physiology **143** (3): 286–292.

Greenberg, J.A., Dobrowski, S.Z., Ramirez, C.M., Tull, J.L. & Ustin, S.L., 2006: A bottom-up approach to vegetation mapping of the Lake Tahoe Basin using hyperspatial image analysis. – Photogrammetric Engineering and Remote Sensing **72** (5): 581–589.

Hall, P.M., 1981: Remote sensing of Douglas-fir trees newly infested by bark beetles. – Master thesis, University of British Columbia, Vancouver, BC, Canada.

Hastie, T., Tibshirani, R. & Friedman, J., 2009: The elements of statistical learning: Data mining, inference, and prediction. – Second Edition, 768 S., Springer, New York, NY, USA.

Heath, J., 2001: The detection of mountain pine beetle green attacked lodgepole pine using Compact Airborne Spectrographic Imager (CASI) data. – Master thesis, University of British Columbia, Vancouver, BC, Canada.

Heller, R., 1968: Previsual detection of ponderosa pine trees dying from bark beetle attack. – Fifth Symposium on Remote Sensing of Environment: 387–434, University of Michigan, USA.

Immitzer, M., Atzberger, C. & Koukal, T., 2012a: Tree species classification with Random Forest using very high spatial resolution 8-band WorldView-2 satellite data. – Remote Sensing **4** (9): 2661–2693.

Immitzer, M., Atzberger, C. & Koukal, T., 2012b: Eignung von WorldView-2 Satellitenbildern für die Baumartenklassifizierung unter besonderer Berücksichtigung der vier neuen Spektralkanäle. – PFG – Photogrammetrie, Fernerkundung, Geoinformation **2012** (5): 573–588.

Kilian, W., Müller, F. & Starlinger, F., 1994: Die forstlichen Wuchsgebiete Österreichs – Eine Naturraumgliederung nach waldökologischen Gesichtspunkten. 60 S., Forstliche Bundesversuchsanstalt, Wien, Österreich.

Krehan, H., 2008: Das ABC der Borkenkäferbekämpfung an Fichte. – Borkenkäfer, BFW Praxis Information **17**: 17–18, http://bfw.ac.at/030/pdf/1818_pi17.pdf (24.9.2011).

Kuhn, M., Wing, J., Weston, S., Williams, A., Keefer, C., Engelhardt, A. & Cooper, T., 2013: caret: Classification and Regression Training. R package version 6.0-30. http://cran.r-project.org/package=caret (7.7.2014).

Lausch, A., Heurich, M., Gordalla, D., Dobner, H.-J., Gwillym-Margianto, S. & Salbach, C., 2013: Forecasting potential bark beetle outbreaks based on spruce forest vitality using hyperspectral remote-sensing techniques at different scales. – Forest Ecology and Management **308**: 76–89.

Lawrence, R. & Labus, M., 2003: Early Detection of Douglas-Fir Beetle Infestation with Subcanopy Resolution Hyperspectral Imagery. – Western Journal of Applied Forestry **18** (3): 202–206.

Leckie, D.G., Tinis, S., Nelson, T., Burnett, C., Gougeon, F.A., Cloney, E. & Paradine, D., 2005: Issues in species classification of trees in old growth conifer stands. – Canadian Journal of Remote Sensing **31** (2): 175–190.

Liaw, A. & Wiener, M., 2002: Classification and regression by randomForest. – R news **2** (3): 18–22.

Marx, A., 2010: Erkennung von Borkenkäferbefall in Fichtenreinbeständen mit multi-temporalen RapidEye-Satellitenbildern und Datamining-Techniken. – PFG – Photogrammetrie, Fernerkundung, Geoinformation **2010** (4): 243–252.

Meddens, A.J.H., Hicke, J.A., Vierling, L.A. & Hudak, A.T., 2013: Evaluating methods to detect bark beetle-caused tree mortality using single-date and multi-date Landsat imagery. – Remote Sensing of Environment **132:** 49–58.

Meigs, G.W., Kennedy, R.E. & Cohen, W.B., 2011: A Landsat time series approach to characterize bark beetle and defoliator impacts on tree mortality and surface fuels in conifer forests. – Remote Sensing of Environment **115** (12): 3707–3718.

Netherer, S. & Nopp-Mayr, U., 2005: Predisposition assessment systems (PAS) as supportive tools in forest management – rating of site and stand-related hazards of bark beetle infestation in the High Tatra Mountains as an example for system application and verification. – Forest Ecology and Management **207** (1–2): 99–107.

Netherer, S. & Schopf, A., 2010: Potential effects of climate change on insect herbivores in European forests – General aspects and the pine processionary moth as specific example. – Forest Ecology and Management **259** (4): 831–838.

Ortiz, S., Breidenbach, J. & Kändler, G., 2013: Early Detection of Bark Beetle Green Attack Using TerraSAR-X and RapidEye Data. – Remote Sensing **5** (4): 1912–1931.

Overbeck, M. & Schmidt, M., 2012: Modelling infestation risk of Norway spruce by Ips typographus (L.) in the Lower Saxon Harz Mountains (Germany). – Forest Ecology and Management **266:** 115–125.

Padwick, C., Deskevich, M., Pacifici, F. & Smallwood, S., 2010: WorldView-2 Pan-Sharpening. – ASPRS 2010 Annual Conference, San Diego, CA, USA.

Pal, M., 2005: Random forest classifier for remote sensing classification. – International Journal of Remote Sensing **26:** 217–222.

R Core Team, 2013: R: A language and environment for statistical computing. – R Foundation for Statistical Computing, Vienna, Austria. – http://www.r-project.org/ (7.7.2014).

Roberts, A., Dragicevic, S., Northrup, J., Wolf, S., Li, Y. & Coburn, C., 2003: Mountain pine beetle detection and monitoring: remote sensing evaluations. – BC Forest Innovation Investment Operational Research Report with Reference to Recipient Agreement R2003-0205. – http://homepage.agrl.ethz.ch/sewolf/PDF/MPB_ForestInovationInvestment-Report_2003.pdf (22.6.2011).

Rodríguez-Galiano, V.F., Chica-Olmo, M., Abarca-Hernandez, F., Atkinson, P.M. & Jeganathan, C., 2012: Random Forest classification of Mediterranean land cover using multi-seasonal imagery and multi-seasonal texture. – Remote Sensing of Environment **121:** 93–107.

Rossi, J.-P., Samalens, J.-C., Guyon, D., van Halder, I., Jactel, H., Menassieu, P. & Piou, D., 2009: Multiscale spatial variation of the bark beetle Ips sexdentatus damage in a pine plantation forest (Landes de Gascogne, Southwestern France). – Forest Ecology and Management **257** (7): 1551–1557.

Rouse, J., Haas, R., Schell, J. & Deering, D., 1973: Monitoring vegetation systems in the Great Plains with ERTS. – Third ERTS symposium, NASA SP-351: 309–317, Washington, DC, USA.

Schelhaas, M.-J., Nabuurs, G.-J. & Schuck, A., 2003: Natural disturbances in the European forests in the 19th and 20th centuries. – Global Change Biology **9** (11): 1620–1633.

Schlerf, M., Atzberger, C., Hill, J., Buddenbaum, H., Werner, W. & Schüler, G., 2010: Retrieval of chlorophyll and nitrogen in Norway spruce (Picea abies L. Karst.) using imaging spectroscopy. – International Journal of Applied Earth Observation and Geoinformation **12** (1): 17–26.

Seidl, R., Schelhaas, M.-J. & Lexer, M.J., 2011: Unraveling the drivers of intensifying forest disturbance regimes in Europe. – Global Change Biology **17** (9): 2842–2852.

Sharma, R., 2007: Using multispectral and hyperspectral satellite data for early detection of mountain pine beetle damage. – PhD thesis, University of British Columbia, Vancouver, BC, Canada.

Sims, D.A. & Gamon, J.A., 2002: Relationships between leaf pigment content and spectral reflectance across a wide range of species, leaf structures and developmental stages. – Remote Sensing of Environment **81** (2–3): 337–354.

Skakun, R.S., Wulder, M.A. & Franklin, S.E., 2003: Sensitivity of the thematic mapper enhanced wetness difference index to detect mountain pine beetle red-attack damage. – Remote Sensing of Environment **86** (4): 433–443.

Stone, C., Chisholm, L. & Coops, N., 2001: Spectral reflectance characteristics of eucalypt foli-

age damaged by insects. – Australian Journal of Botany **49** (6): 687–698.

Tomiczek, C., Cech, T.L., Fürst, A., Hoyer-Tomiczek, U., Krehan, H., Perny, B. & Steyrer, G., 2011: Forest Protection Situation 2010 in Austria (in German with English summary). – Forstschutz aktuell **52:** 3–9.

Toscani, P., Immitzer, M. & Atzberger, C., 2013: Texturanalyse mittels diskreter Wavelet Transformation für die objektbasierte Klassifikation von Orthophotos. – PFG – Photogrammetrie, Fernerkundung, Geoinformation **2013** (2): 105–121.

Updike, T. & Comp, C., 2010: Radiometric use of WorldView-2 imagery. – DigitalGlobe, Longmont. – http://www.digitalglobe.com/downloads/Radiometric_Use_of_WorldView-2_Imagery.pdf (7.5.2012).

Venables, W.N. & Ripley, B.D., 2002: Modern applied statistics with S. – Fourth Edition, 495 S., Springer, New York, NY, USA.

Waser, L.T., Küchler, M., Jütte, K. & Stampfer, T., 2014: Evaluating the Potential of WorldView-2 Data to Classify Tree Species and Different Levels of Ash Mortality. – Remote Sensing **6** (5): 4515–4545.

Wulder, M.A., Dymond, C.C. & Erickson, B., 2004: Detection and monitoring of the mountain pine beetle – Information Report BC-X-398. Canadian Forest Service, Victoria, BC, Canada. – http://www.for.gov.bc.ca/hfd/library/documents/bib92565.pdf (15.9.2011).

Wulder, M.A., Dymond, C.C., White, J.C., Leckie, D.G. & Carroll, A.L., 2006a: Surveying mountain pine beetle damage of forests: A review of remote sensing opportunities. – Forest Ecology and Management **221** (1–3): 27–41.

Wulder, M.A., White, J.C., Bentz, B., Alvarez, M.F. & Coops, N.C., 2006b: Estimating the probability of mountain pine beetle red-attack damage. – Remote Sensing of Environment **101** (2): 150–166.

Wulder, M.A., White, J.C., Carroll, A.L. & Coops, N.C., 2009: Challenges for the operational detection of mountain pine beetle green attack with remote sensing. – Forestry Chronicle **85** (1): 32–38.

Addresses of the Authors:

Markus Immitzer & Clement Atzberger, University of Natural Resources and Life Sciences, Vienna (BOKU), Institute of Surveying, Remote Sensing and Land Information, Peter-Jordan-Straße 82, A-1190 Vienna, Tel.: +43-1-47654-5100, Fax: +43-1-47654-5142, e-mail: {markus.immitzer}{clement. atzberger}@boku.ac.at